Drug Design, Development and Therapy

Dovepress
Taylor & Francis Group

Open Access Full Text Article

ORIGINAL RESEARCH

Exploring the Therapeutic Mechanism of Jianpi Zhidong Decoction on Tourette Syndrome Based on Proteomics and Network Pharmacology

Ning Zhang[1,*], Hongxian Zhang[1,*], Jianning Guo[2], Yaluan Ma[3], Xue Bai[1], Ning Ma[1], Xiaoxiao Ji[1], Yanli Meng[1], Huifang Li[1], Tananan Sangwanit[1], Yixin Shi[1], Jing Zhao[1], Xiang Li[1], Jingyuan Lin[1], Xia Cui[1]

[1]Pediatric Department, Beijing University of Chinese Medicine Third Affiliated Hospital, Beijing, People's Republic of China; [2]Pediatric Department, China-Japan Friendship Hospital, Beijing, People's Republic of China; [3]Laboratory of Molecular Biology, Institute of Basic Theory of Traditional Chinese Medicine, China Academy of Chinese Medical Sciences, Beijing, People's Republic of China

*These authors contributed equally to this work

Correspondence: Xia Cui, Department of Pediatrics, Beijing University of Chinese Medicine Third Affiliated Hospital, No. 51 Xiaoguan Street, Andingmen Wai, Chaoyang District, Beijing, 100029, People's Republic of China, Email cuixia68@163.com

Purpose: To explore the pharmacological effects of Jianpi Zhidong Decoction (JPZDD) on Tourette Syndrome (TS) using proteomics and network pharmacology.

Materials and Methods: Chemical components of JPZDD were identified via UPLC-MS/MS. Chronic restraint stress TS model was established by intraperitoneal injection of iminodipropionitrile (IDPN) for 1 week with restraint stress for 3 weeks. Sixty male SD rats were divided into control, model, Tiapride (Tia), and JPZDD groups. After the intervention of 28 days, behavioral tests, Nissl staining, Western blot, immunofluorescence, colorimetry, and ELISA were performed to evaluate the pharmacological effects of JPZDD. Proteomics and network pharmacology predicted targets, validated by Western blot.

Results: JPZDD alleviated stereotypic behaviors, hippocampal pathology, and modulated glucose metabolites (GLU, pyruvate, lactate, ATP). It downregulated GLUT1, GLUT3, HK2, and LDHA levels while upregulating PDHA level. Besides, JPZDD balanced M1/M2 microglial phenotypes, reducing IL-1β and IL-6 and increasing IL-4 and IL-10. UPLC-MS/MS identified 44 active ingredients and 123 targets; proteomics revealed 28 differentially expressed proteins. GO/KEGG analysis implicated that the PI3K/AKT/mTOR pathway may be the molecular target. JPZDD inhibited PI3K, AKT, and mTOR phosphorylation.

Conclusion: JPZDD (16 $g \cdot kg^{-1} \cdot d^{-1}$) alleviates motor tics, modulates microglial activation and glucose metabolism, and downregulates the PI3K/AKT/mTOR pathway, providing a mechanistic basis for its therapeutic role in TS.

Keywords: Tourette syndrome, Jianpi Zhidong decoction, glucose metabolism, microglia, network pharmacology

Introduction

Tourette Syndrome (TS) is a prevalent chronic neuropsychiatric disorder characterized by motor and vocal tics, predominantly affecting children, with a significant population impacted in China. The prevalence of tic disorder was 2.5%, with a significantly higher rate observed in boys compared to girls.[1] Chronic stress is widely acknowledged as a key trigger for TS, contributing to symptom exacerbation given the condition's sensitivity to stressors stemming from social, psychological, and emotional pressures.[2] The pathogenesis of TS is multifactorial, involving dysregulation of neurotransmitter systems within the cortico-striato-thalamo-cortical (CSTC) circuitry, genetic predisposition, immune dysfunction, environmental factors (such as perinatal complications, familial aggregation of neuropsychiatric disorders, and recurrent respiratory infections), and psychosocial influences.[3] Emerging evidence indicates persistent neuroinflammatory changes and aberrant microglial activation within the central nervous system of patients with Tourette syndrome, concomitant with impaired glucose metabolism in the hippocampal complex.[4,5] The disruption of glucose metabolism is frequently linked to various nervous system disorders. Microglia, as the primary immune cells in the central nervous

Received: 25 November 2024
Accepted: 8 April 2025
Published: 23 April 2025

Graphical Abstract

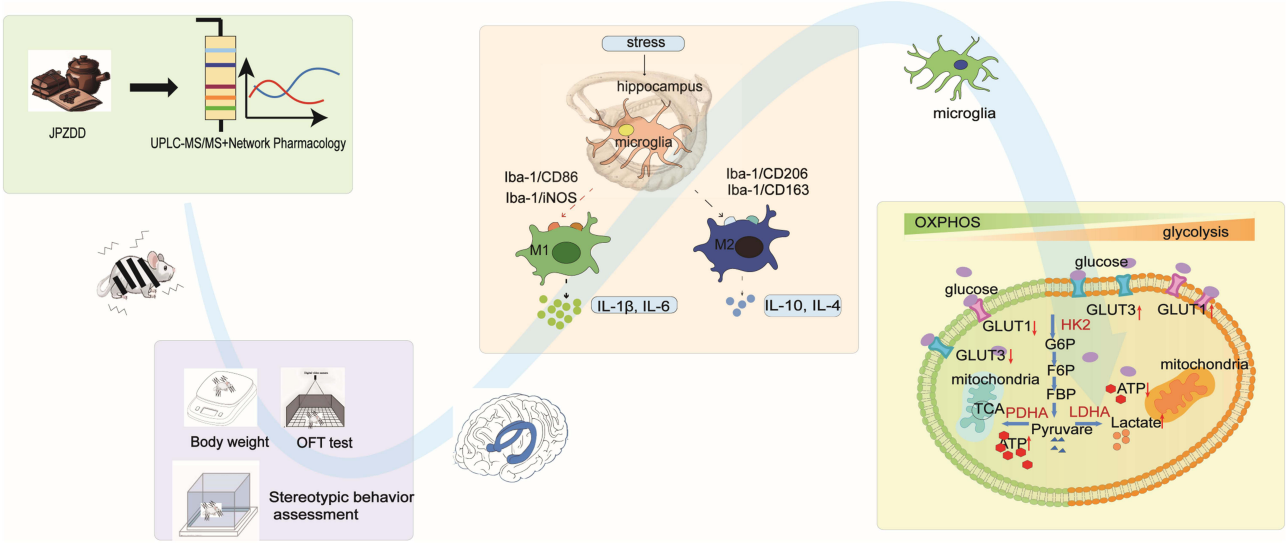

system, have substantial energy demands for releasing inflammatory cytokines and performing phagocytosis, with glucose serving as their primary energy source.[6,7] The interplay between glucose metabolism and microglia activation-mediated inflammation is apparent.[8] Stressors induce a metabolic reprogramming in microglia, adjusting their metabolic profile to meet energy demands,[9,10] thus altering their phenotype and function. The transition from oxidative phosphorylation to glycolysis is a defining feature of microglia activation towards the pro-inflammatory M1 phenotype, and a key driver of neuroinflammation.[8,10,11] Under stress conditions, glycolysis escalates, leading to sustained microglia activation, polarization towards the pro-inflammatory M1 phenotype, and exacerbation of neuroinflammation.[12] Consequently, the atypical polarization of microglia and metabolic reprogramming of glucose might be implicated in the pathogenesis of TS.

In the management of Tourette Syndrome (TS), psychopharmacological interventions face limitations in efficacy and tolerability,[13] while neurobehavioral therapy's implementation in China is constrained by accessibility and cultural factors. Traditional Chinese Medicine (TCM) offers distinct advantages, with emerging evidence demonstrating that Jianpi Zhidong Decoction (JPZDD) exhibits significant therapeutic efficacy. JPZDD has been shown to have an effect on TS, revealing JPZDD's potential in alleviating behavioral dysfunction and brain mitochondrial dysfunction, keeping the balance of neurotransmitters, such as dopamine(DA), norepinephrine(NE), glutamic acid(GLU), gamma-aminobutyric acid(GABA), enhancing neuroprotection, improving cognitive function, and alleviating stress.[14–18] Moreover, JPZDD has effect on different brain areas, including hippocampus, striatum, prefrontal cortex,[19–21] and has good safety and good long-term efficacy.[15] Some researchers believed that JPZDD could resist the influence of stress factors by regulating the function of HPA axis.[14] But its precise therapeutic mechanisms remain unclear. In this paper, the chemical components of JPZDD were detected by UPLC-MS/MS, and the potential targets of JPZDD for treating TS were explored through network pharmacology and proteomics. In addition, its therapeutic effect was subsequently verified in animal experiments, providing a new idea for further research of JPZDD.

Materials and Methods

Chemicals

GLUT1 antibody (batch number: 21829-1-AP), GLUT3 antibody (batch number: 20403-1-AP), CD86 antibody (batch number: 13395-1-AP), Tubulin-Alpha Antibody (batch number: 66031-1-Ig), HRP-conjugated Affinipure Goat Anti-

Rabbit IgG (H + L) (1:10000, batch number:SA00001-2), HRP-conjugated Affinipure Goat Anti-Mouse IgG (H + L) (1:10000, batch number:SA00001-1) were purchased from proteintech; anti-Hexokinase II antibody (batch number: ab209847), anti-PDHA1antibody (batch number: ab168379), anti-Lactate Dehydrogenase antibody (batch number: ab52488), anti-Iba1 antibody (batch number: ab283319), anti-PI3 Kinase p85 alpha antibody (batch number: ab191606), Anti-PI 3 Kinase p85 alpha (phospho Y607) antibody (batch number: ab182651), anti-AKT1 + AKT2 + AKT3 antibody (batch number: ab179463), anti-AKT1 (pS473) + AKT2 (pS474) + AKT3 (pS472) antibody (batch number: ab192623), anti-mTOR antibody (batch number: ab134903), anti-mTOR (phospho S2481) antibody (batch number: ab137133) were purchased from Abcam; Lactic Acid assay kit (batch number: RGB-40022), Pyruvate assay kit (batch number: RGB- 40071), Glucose Kit (batch number: RGB-30001), IL-1β enzyme linked immunosorbent assay kit (batch number: RGB- 60013R), IL-6 enzyme linked immunosorbent assay kit (batch number: RGB- 60023R), IL-4 enzyme linked immunosorbent assay kit (batch number: RGB- 60021R), IL-10 enzyme linked immunosorbent assay kit (batch number: RGB- 60026R) were purchased from Beijing Rgbos Technology Development Co., LTD (Beijing, China); CD206 antibody (batch number: 24595T) was purchased from Cell Signaling Technology; anti-iNOS antibody (batch number: GB11119-100), anti-CD163 antibody (batch number: GB11340-100) were purchased from Wuhan Servicebio Technology Co., Ltd (Wuhan, China); super ECL Plus hypersensitive Chemiluminescence Solution (batch number: P1050) was purchased from Applygen.

Preparation of JPZDD

JPZDD granules were provided by the Pharmacy Department of the Third Affiliated Hospital of Beijing University of Chinese Medicine (Beijing, China) according to the methods provided in our previous study[22] (Table 1). A pair of JPZDD granule was dissolved in 50 mL of distilled water, after well-mixed, the solution was stored at 4 °C before use.[20]

Chemical Profiling of JPZDD

Ultra performance liquid chromatography tandem mass spectrometry was used to identify chemical compounds containing JPZDD. Detailed information on the instrument parameters and the gradient elution program are provided in Supplementary Section 1.

Animals

Male Sprague Dawley rats (n = 60, 3 weeks old, 50 ± 10 g) were purchased from Beijing Jinmuyang Experimental animal breeding Co., LTD (SCXK 2019–0010, Beijing, China). The rats were housed under controlled conditions at a temperature of 20 °C - 26 °C with humidity of 40% - 70%.

Grouping, Modeling and Treatment

One week after adaptive feeding, 60 male rats were divided into a control group (n = 15) and a modeling group (n = 45) at random. The modeling group received IDPN (250 mg·kg-1 ·d-1) intraperitoneal injection once daily for 7 consecutive

Table 1 The List of Herbal Compositions in JPZDD

Herbal Name	Herbal Name in Chinese	Dosage
Angelica sinensis (Oliv.) Diels	Danggui	10 g
Citrus reticulata Blanco	Chenpi	6 g
Atractylodes macrocephala Koidz.	Baizhu	10 g
Pinellia ternata (Thunb.) Makino	Banxia	6 g
Gentiana scabra Bunge	Longdan	3 g
Ligusticum striatum DC.	Chuanxiong	6 g
Saposhnikovia divaricata (Turcz.) Schischk.	Fangfeng	6 g
Pseudostellaria heterophylla (Miq.) Pax	Taizishen	10 g
Poria cocos (Schw.) Wolf.	Fuling	10 g
Uncaria rhynchophylla (Miq.) Miq. ex Havil.	Gouteng	10 g

days combined with chronic restraint for 21 consecutive days. The control group was given with 0.9% saline (250 mg·kg-1 ·d-1) by intraperitoneal injection. After 21 days, the modeling groups were further categorized into three groups: model group (n = 15), Tiapride (Tia) group (n = 15), and JPZDD group (n = 15), based on their stereotypical behavior scores. Rats in the control group and model groups were given distilled water (10 mL·kg-1 ·d-1), while those in the Tia and JPZDD groups were given tiapride suspension (21 mg·kg-1 ·d-1, 4.2 × clinical equivalent dose) and JPZDD granule solution (16 g·kg-1 ·d-1,4.2 × clinical equivalent dose), respectively. The optimal dose has been confirmed in the Preliminary study.[23] Therefore, only the optimal dose was used in this study, and no dose exploration was carried out. All were given gavage for 28 days (Figure 1).

Behavior Analysis

Stereotypic behavior assessment involved observing the rats for 5 minutes following a 5-minute acclimatization period. This observation was conducted for 7 days in a double-blind manner. Stereotypic behavior was scored according to the previous study.[24] Following each rat's assessment, the cage was thoroughly cleaned to prevent any potential influence on the subsequent rats.

Open-field test was maintained in low light and low noise conditions, with each rat placed at the center of the open field for video recording and timed observations. Utilizing a motion tracking analysis system, we analyzed the rat's movement patterns over a 5-minute period. Key parameters measured included total distance traveled, average speed, central distance, center time before and after gavage administration.

Nissl Staining

Dissected the fresh brain tissue and immediately put it into 4% paraformaldehyde for 48 h. The tissues were then dehydrated, paraffin-embedded, and sliced into 5 μm paraffin sections. Paraffin sections were stained with toluidine blue solution to observe the morphological and pathological changes under the light microscope (Nikon E400, Tokyo, Japan).

Western Blotting

Hippocampus tissues were weighed and homogenized using a lysis buffer containing 10% protease and phosphatase inhibitors to extract total proteins. The Supernatant was obtained for the assay. The BCA method was adopted to measure protein concentration. Equivalent protein (30 μg) samples were heat denatured at 100 °C for 10 min. Constant-voltage electroporation was performed, and the samples were blocked with 5% skimmed milk powder at room temperature for 2 h. After TBST rinsing, the samples were mixed with antibodies at 4 °C overnight. The membranes were washed and incubated with the secondary antibodies for 1h in the dark. Membranes were then washed and incubated with super ECL

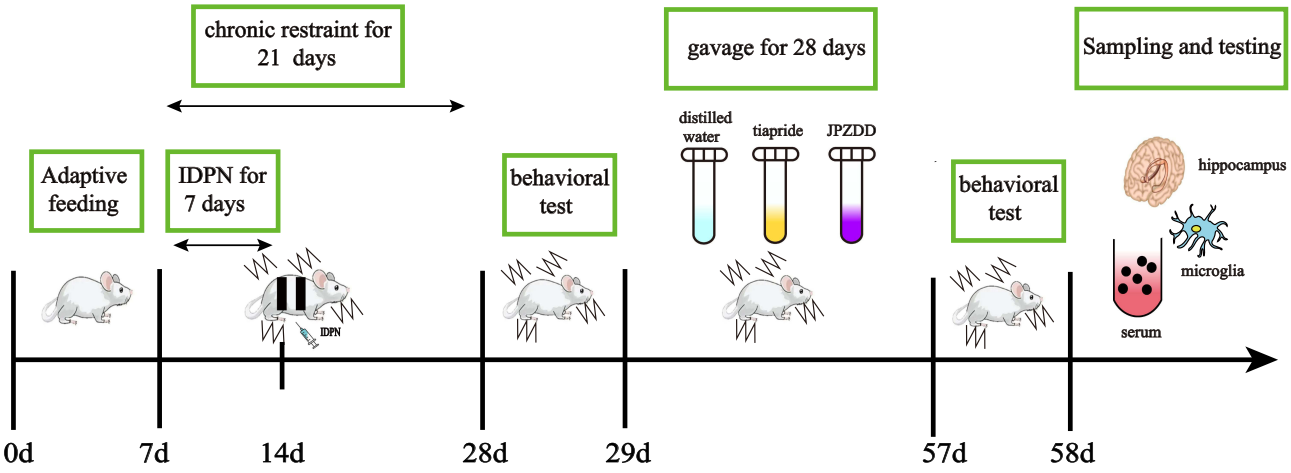

Figure 1 Flow chart of animal studies.

Plus hypersensitive chemiluminescence solution. Afterward, protein bands were visualized and measured using c600 ultra-sensitive multifunctional imager (Azure Biosystems, USA). Images were analyzed with Image J.

Immunohistochemistry and Immunofluorescence Analysis

5 μm-paraffin sections were immersed in sodium citrate, then incubated in endogenous peroxidase blocker, and then blocked with goat serum. Later, the sections were incubated overnight at 4°C with the primary antibodies. After washing with PBS, the sections were incubated with the corresponding secondary antibody. For immunohistochemistry, sections need to be followed by DAB color development, hematoxylin counterstaining, and sealing with neutral gum after dehydration. The brown-yellow particles were positively expressed under the light microscope. For immunofluorescence, nuclear stained with DAPI (Blue). We imaged hippocampal sections using a fluorescence scanner (Olympus, Japan) and a confocal microscope (Leica, Germany).

Measurement of ATP, GLU, LD, Pyruvate, IL-1β, IL-6, IL-4, IL-10 Levels in Hippocampus

Hippocampus were frozen at −80 °C after sample collection. The levels of ATP, GLU, LD, Pyruvate, IL-1β, IL-6, IL-4 and IL-10 were measured following the kit instructions.

Network Pharmacology Analysis

The chemical components of JPZDD were identified by UPLC-MS/MS. Based on ADME-related properties (absorption, distribution, metabolism, and excretion), we screened the chemical components of JPZDD in the TCMSP database (https://tcmsp-e.com/index.php). The screening criteria were oral bioavailability (OB) ≥ 30% and drug-likeness (DL) ≥ 0.18. Afterwards, the canonical SMILES of each chemical component was obtained from PubChem (https://pubchem.ncbi.nlm. nih.gov/) and then those SMILES were imported into the Swiss Target Prediction (http://www.swisstargetprediction.ch/).[25] Repetitive chemical components were removed to establish the potential target database of JPZDD.

GeneCards database was searched using the keywords "Tourette syndrome", and the species was defined as "Homo sapiens", and the "probability" > 0 was used as the screening condition to predict the action targets of those compounds. We compared and analyzed potential targets of JPZDD with disease targets to identify potential treatment genes. A Venn diagram was created using a bioinformatics platform to visualize the common overlapping genes (http://www.bioinformatics.com.cn/).

Construction of the Protein-Protein Interaction (PPI) Network

The overlapping genes were inputted into the STRING database (https://www.string-db.org/) to build the protein interaction network. Subsequently, the protein interaction data was imported into Cytoscape software (version 3.9.1) to visually represent the interactions within the PPI network.

Gene Ontology (GO) Enrichment and Pathway Analysis

Gene Ontology (GO) functional enrichment analysis and Kyoto Encyclopedia of Genes and Genomes (KEGG) pathway enrichment analysis were performed on DAVID V6.8 database to predict potential targets of JPZDD for the treatment of TS. We performed gene function annotation on the potential target genes using three GO modules: Biological Process (BP), Molecular Function (MF), and Cellular Component (CC). Pathway enrichment analysis was conducted to predict the potential biological functions and molecular pathways modulated by JPZDD.

Proteomics Analysis

Extracted proteins were labeled by tandem mass tag (TMT) for proteomic analysis of rat hippocampus. Combined LC-MS/MS analysis was performed by Shanghai Majorbio Bio-Pharm Technology Co., Ltd (Shanghai, China). Data were analyzed using

the free online Majorbio Cloud Platform (www.majorbio.com). GO and KEGG analyses were performed enrichment evaluation. Detailed information on the instrument and program parameters are provided in Supplementary Section 2.

Statistical Analyses

Statistical analysis was performed using GraphPad Prism 9.0 software. Data were presented as mean ± standard deviation. One-way analysis of variance (ANOVA) was used for multiple group comparisons. $p < 0.05$ was considered statistically significant.

Results

Analysis of the Chemical Composition of JPZDD

The chemical components of JPZDD were analyzed by UPLC-MS/MS, with mass spectrometric data processed through Analyst 1.6.3 software. The total ions current (TIC) of the mixed quality control samples represented the cumulative intensities of all ions in the mass spectrum at each time point. A total of 2242 compounds were identified (Supplementary Table 1). The Class I metabolites consisted of amino acids and their derivatives, phenolic acids, nucleotides and their derivatives, flavonoids, etc (Figure 2). The chemical components of JPZDD were identified using UPLC-MS/MS, with 44 chemical components screened based on the TCMSP database on specific criteria (OB ≥ 30% and DL ≥ 0.18) (Table 2).

JPZDD Improves Behavioral Performance in Chronic Restraint Stress TS Rats

The weight change of rats were tested every 7 days and the result was shown in Figure 3A. The model rats exhibited decreased weight compared to the control group. Moreover, chronic restraint stress TS model led to varying degrees of abnormal stereotypic behaviors compared to the control group ($p < 0.001$). Following 28 days of gavage, the JPZDD group demonstrated significantly lower stereotype scores than both the model and Tia group ($p < 0.001$) (Figure 3B). The OFT served to detect anxiety-depressive behaviors indicative of stress state. In comparison to the control group, measures such as total distance, average speed, central distance and central time were elevated in JPZDD group ($p < 0.05$) (Figure 3C–F).

JPZDD Improves Histopathology in Hippocampus

Nissl staining revealed in the CA1, CA3, and DG regions, the nerve cell morphology exhibited intact structure and orderly arrangement with abundant Nissl granules in the control group. There were basically no pathological changes such as vacuoles and pyknosis. Conversely, in the model group, neuronal nuclei displayed pyknosis or disappearance, reduced volume, looseness, disorganization, with blurred edges and diminished Nissl granules compared to the control. After administration, the rats treated with Tiapride and JPZDD exhibited increased Nissl granule count in the hippocampus, deepened coloration, partially restored cell membrane integrity, and clearer nuclei. These findings suggest JPZDD's efficacy in ameliorating hippocampal neuron damage of chronic restraint stress TS rats (Figure 4).

JPZDD Affects Glucose Metabolism in Hippocampus of Chronic Restraint Stress TS Rats

Glucose metabolites were measured after 28 days of continuous drug administration. Compared with control group, the hippocampal ATP levels were significantly reduced in the model group, while GLU, Pyruvate, and LD levels were elevated ($p < 0.05$). After 28 days of administration, ATP level in Tia group and JPZDD group increased compared with model group, with the JPZDD group demonstrating a statistically significant difference ($p < 0.05$) (Figure 5A–D). Western blotting analysis was conducted to evaluate the expression of GLUT1, GLUT3, HK2, LDHA, and PDHA proteins. Results indicated elevated expression levels of GLUT1 and GLUT3 in the hippocampus of rats in the model group compared to the control group ($p < 0.05$). Conversely, in the JPZDD group, GLUT1 and GLUT3 protein levels were reduced compared to the model group ($p < 0.05$) (Figure 5E–G). The expression of HK2 and LDHA protein in hippocampus of rats in model group increased compared with control group ($p < 0.05$), while PDHA expression decreased ($p > 0.05$). Compared with model group, the expression of HK2 protein in JPZDD group decreased ($p < 0.05$), while LDHA and PDHA expression showed a tendency to increase ($p > 0.05$) (Figure 5H–J).

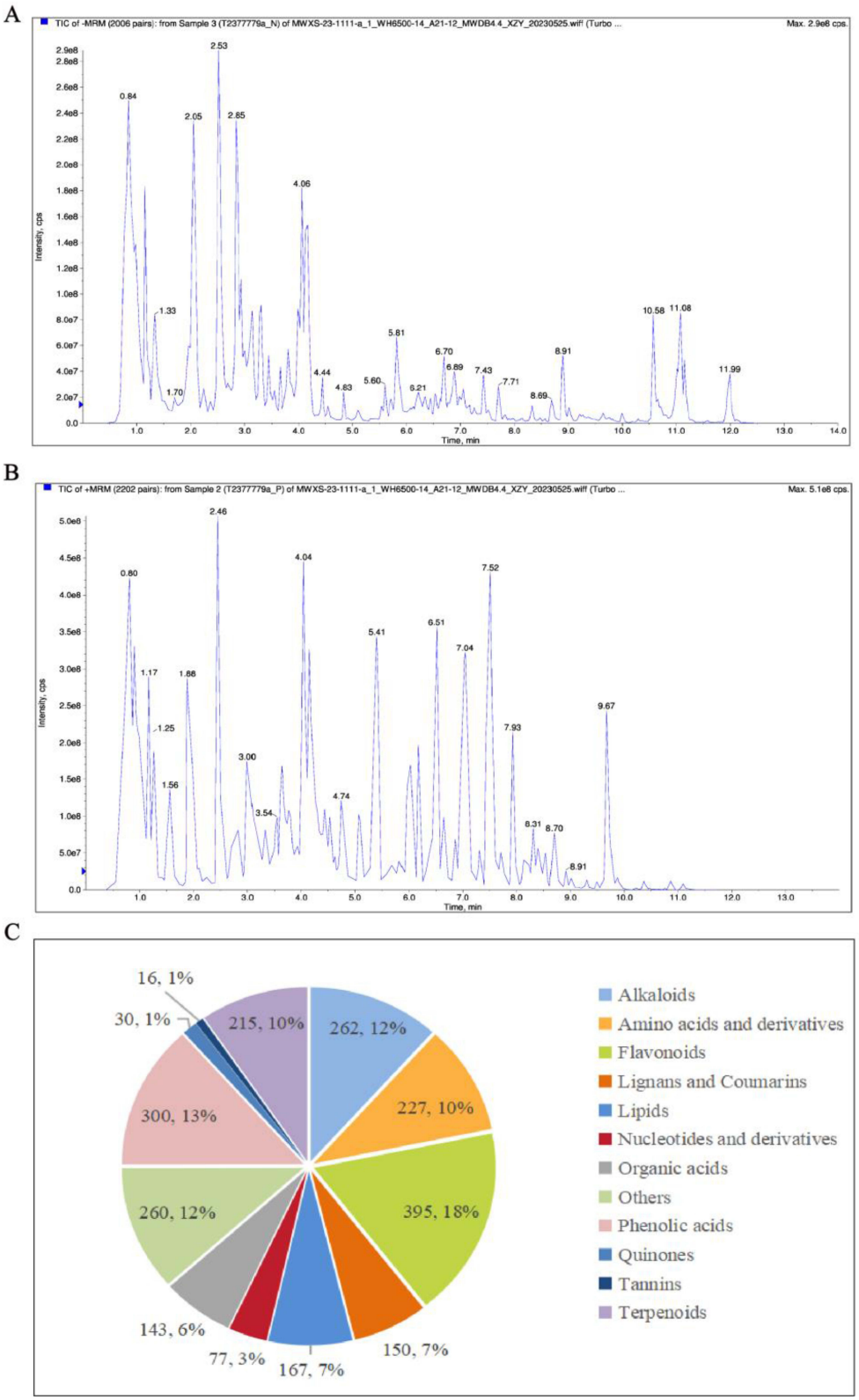

Figure 2 UPLC-MS/MS analysis of the chemical components of JPZDD. (**A**) Chromatogram of the positive ion mode. (**B**) Chromatogram of the negative ion mode. The abscissa shows the retention time (Rt) of the metabolites, and the ordinate shows the ion current intensity, intensity unit: count per second (cps). (**C**) Quantity and proportion of Class I compounds.

https://doi.org/10.2147/DDDT.S505173

Table 2 Compounds of JPZDD

Compounds	Formula	CAS	Molecular weight (Da)	OB (%)	DL
Luteolin	C15H10O6	491–70-3	286.05	36.16	0.25
Acacetin	C16H12O5	480–44-4	284.07	34.97	0.24
1-Linoleoylglycerol	C21H38O4	2277–28-3	354.28	37.18	0.3
Linarin	C28H32O14	480–36-4	592.18	39.84	0.71
Dehydropachymic acid	C33H50O5	77012–31-8	526.37	35.11	0.81
Eburicoic acid	C31H50O3	560–66-7	470.38	38.7	0.81
Poricoic acid A	C31H46O5	137551–38-3	498.33	30.61	0.76
Poricoic acid B	C30H44O5	137551–39-4	484.32	30.52	0.75
Poricoic acid C	C31H46O4	151200–89-4	482.34	38.15	0.75
Gallic acid	C7H6O5	149–91-7	170.02	36.91	0.75
Naringenin	C15H12O5	480–41-1	272.07	59.29	0.21
Prunin	C21H22O10	529–55-5	434.12	59.29	0.21
Naringin	C27H32O14	10236–47-2	580.18	59.29	0.21
Narirutin	C27H32O14	14259–46-2	580.18	59.29	0.21
Hesperidin	C28H34O15	520–26-3	610.19	47.74	0.27
Hesperetin	C16H14O6	520–33-2	302.08	47.74	0.27
Hesperetin-5-O-glucoside	C22H24O11	69651–80-5	464.13	47.74	0.27
Nobiletin	C21H22O8	478–01-3	402.13	61.67	0.52
Baicalein	C15H10O5	491–67-8	270.05	33.52	0.21
Baicalin	C21H18O11	21967–41-9	446.08	40.12	0.75
Eicosenoic acid	C20H38O2	26764–41-0	310.29	30.7	0.2
Xanthosine	C10H12N4O6	146–80-5	284.08	44.72	0.21
Praeruptorin B	C24H26O7	81740–07-0	426.17	59.65	0.66
Imperatorin	C16H14O4	482–44-0	270.09	34.55	0.22
Ledebouriellol	C20H22O7	84272–83-3	374.14	32.05	0.51
Phellopterin	C17H16O5	2543–94-4	300.10	40.19	0.28
Wogonin	C16H12O5	632–85-9	284.07	30.68	0.23
Ethyl linoleate	C20H36O2	544–35-4	308.27	42	0.19
Isoimperatorin	C16H14O4	482–45-1	270.09	45.46	0.23
Decursin	C19H20O5	5928–25-6	328.13	39.27	0.38
Quercetin	C15H10O7	117–39-5	302.04	46.43	0.28
Uncarine C	C21H24N2O4	5629–60-7	368.17	56.74	0.75
Hirsutine	C22H28N2O3	7729–23-9	368.21	32.75	0.64
Rhynchophylline	C22H28N2O4	76–66-4	384.20	41.82	0.57
Uncarine E	C21H24N2O4	5171–37-9	368.17	78.38	0.75
Corynoxine	C22H28N2O4	6877–32-3	384.20	57.85	0.57
Mitraphyllic acid	C20H22N2O4	10126–00-8	354.16	31.7	0.7
Yohimbine	C21H26N2O3	146–48-5	354.19	46.42	0.81
Hirsuteine	C22H26N2O3	35467–43-7	366.19	41.64	0.64
Kaempferol	C15H10O6	520–18-3	286.05	41.88	0.24
Isorhynchophylline	C22H28N2O4	6859–01-4	384.20	47.31	0.57
Corynoxine B	C22H28N2O4	17391–18-3	384.20	54.47	0.57
Isocorynoxeine	C22H26N2O4	51014–29-0	382.19	57.13	0.57
Isovitexin	C21H20O10	38953–85-4	432.11	31.29	0.72

JPZDD Regulates Microglia Polarization and Inflammation

The morphology of hippocampal microglia was observed by immunohistochemistry. In the control group, microglia exhibited small cell bodies with numerous long, branching processes, indicative of an inactive resting state. Hippocampal microglia in the model group were significantly enlarged, and most of them showed a typical "amoebo-like" activation state. Compared with the model group, microglial activation and the expression levels of Iba-1, CD86, and CD206 were

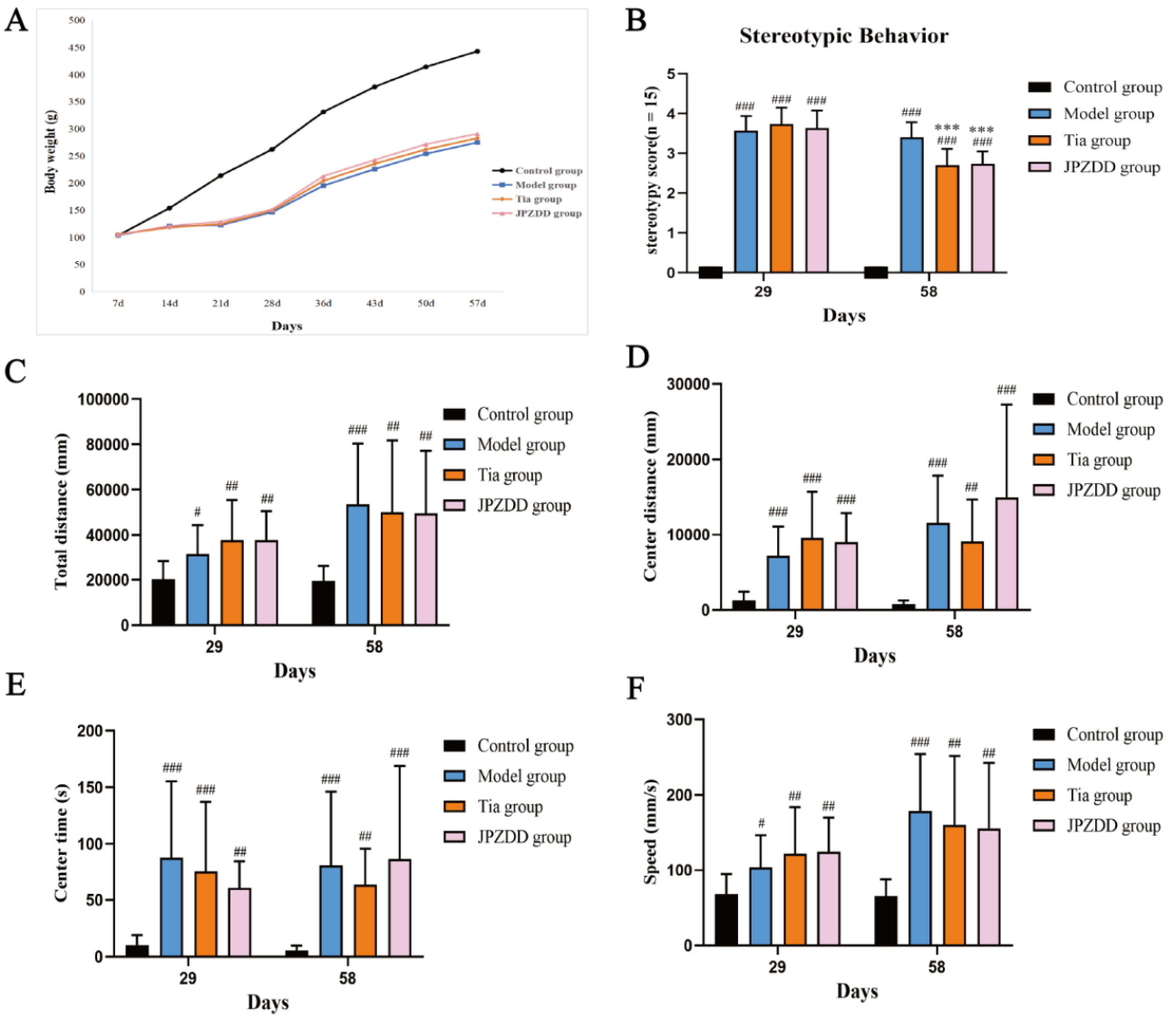

Figure 3 JPZDD had certain efficacy in the treatment of the symptoms of TS. (**A**) Body weight changes of rats in each group (n = 15 per group). (**B**) Evaluations of stereotypic behavior scores (n = 15 per group). (**C–F**) Evaluations of in the open field tests in each group (n = 15 per group). Data are expressed as mean ± SD (post-hoc LSD test). #P < 0.05, ##P < 0.01, ####P < 0.001 vs Control group. ***P < 0.001 vs Model group.

notably reduced in the Tia group and the JPZDD group (Figure 6A). High expression of CD86 is associated with M1-type microglial polarization, promoting a pro-inflammatory response, while high expression of CD206 is linked to M2-type polarization, associated with anti-inflammatory and tissue repair functions. Our results suggest that JPZDD may promote microglial polarization towards the M2 type.

To further verify these findings, we performed triple immunofluorescence staining to examine the polarization of microglia. Compared with the control group, the model group exhibited an increase in the co-localization of Iba-1 with iNOS, indicative of M1-type microglia, and a decrease in the co-localization of Iba-1 with CD163, indicative of M2-type microglia. Following treatment, the Tia group and JPZDD group both demonstrated decreased Iba-1/iNOS co-localization, while Iba-1/CD163 co-localization increased compared to the model group (Figure 6B).

With an increase in M1 type polarization, there was an escalation in the secretion of inflammatory factors. Our observations revealed a significant elevation in IL-1β levels in the model group ($p < 0.05$), while IL-6 had a downward trend ($p > 0.05$), IL-4 and IL-10 were significantly reduced ($p < 0.05$) compared with control group. Compared with model group, the IL-1β level in Tia group and JPZDD group was significantly decreased ($p < 0.05$), while the IL-6 level

https://doi.org/10.2147/DDDT.S505173

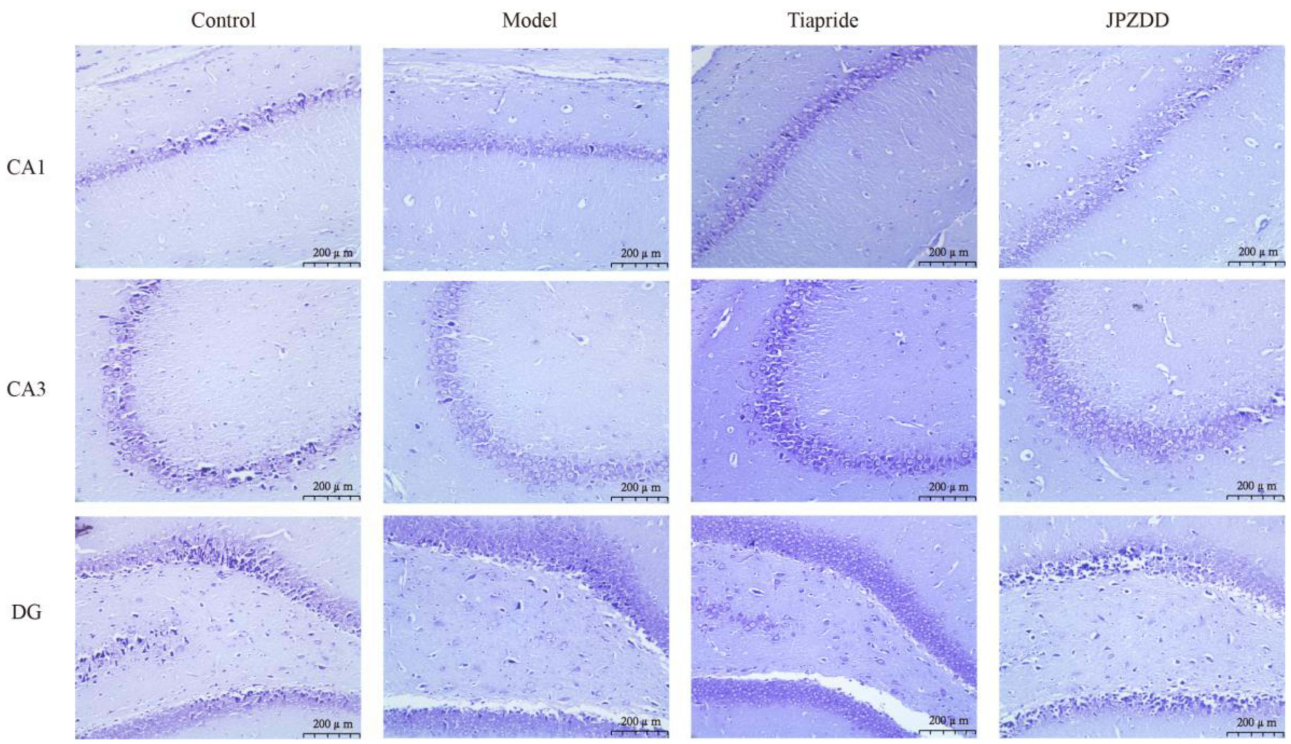

Figure 4 Observed the damage degree of neurons in hippocampus of chronic restraint stress TS rats by Nissl staining (× 200, Scale bars = 200 μm, n = 6 per group).

had a downward trend, the IL-4 and IL-10 levels had an increasing trend ($p > 0.05$) (Figure 6C–F). These findings suggest that JPZDD may effectively modulate excessive inflammatory responses in chronic restraint stress TS rats.

Analysis of Potential Biological Targets Based on Network Pharmacology

In order to further analyze the multi-component multi-target network of traditional Chinese medicine, the potential targets of JPZDD were predicted by means of network pharmacology. A total of 941 potential biological targets of these chemical components were predicted by the SwissTargetPrediction database. Subsequent Venn analysis of these predicted targets and disease-related genes linked to Tourette Syndrome revealed 123 overlapping genes, suggesting potential molecular targets of JPZDD (Figure 7A). The identified gene targets underwent PPI network analysis using the STRING database (Figure 7B). The potential mechanism of JPZDD was visualized by constructing a composite target network using Cytoscape software, comprising 168 nodes and 393 edges (Figure 7C).

Utilizing the DAVID platform, GO and KEGG pathway enrichment analyses were conducted to further explore the molecular mechanisms underlying JPZDD's intervention in TS. GO enrichment analysis highlighted significant involvement in BP, such as chemical synaptic transmission, G protein-coupled receptor signaling pathway, coupled cyclic nucleotide second messenger, phospholipase C-activated G protein-coupled receptor signaling pathway, and the CC including components of the plasma membrane, synapses, plasma membranes. MF encompassed neurotransmitter receptor activity, G protein-coupled serotonin receptor activity, serotonin binding (Figure 7D). KEGG pathway analysis indicated potential involvement in pathways such as neuroactive ligand-receptor interaction pathway, serotonin-activated synaptic pathway, cAMP pathway, dopamine-related pathway, and PI3K-AKT signaling pathway (Figure 7E).

Proteomics Analysis

To identify the targets of JPZDD, we performed proteomics to screen for differential proteins among control group, model group and JPZDD group. A total of 22525 proteins were identified (Supplementary Table 2), of which 28 were significantly differentially expressed between model group and JPZDD group ($p > 0.05$), including 11 up-regulated proteins and 17 down-regulated proteins (Figure 8A). The Bubble chart depicted the involvement of DEPs in the

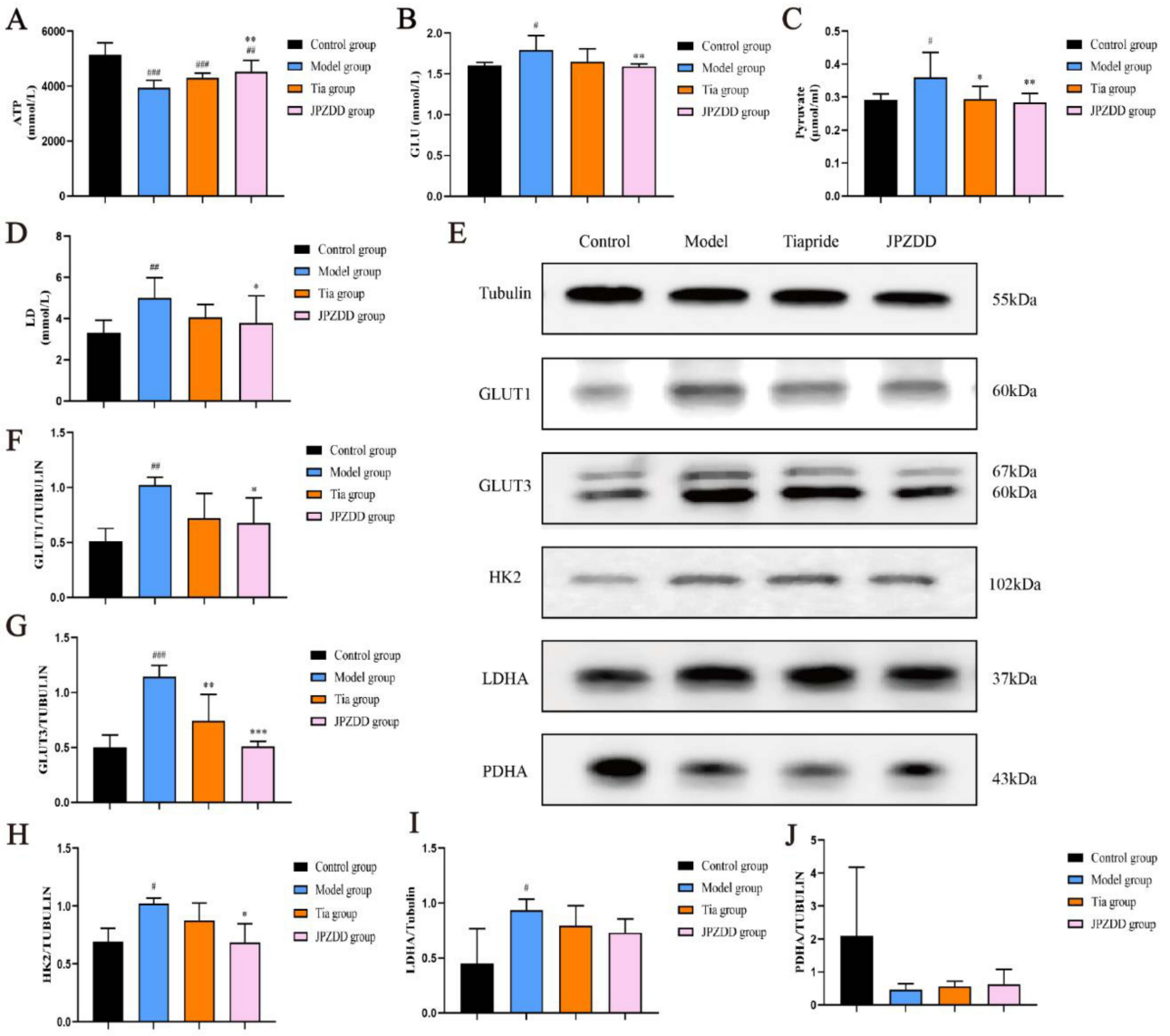

Figure 5 Hippocampus levels of glucose metabolites and glucose metabolizing enzymes in different groups. (**A–D**) The levels of GLU, Pyruvate and LD in hippocampus (n = 6 per group). (**E**) GLUT1,GLUT3, HK2, LDHA and PDHA proteins expressions in hippocampal tissue after treatment for 28 days were determined by Western blotting assay. Tubulin was used as an internal control (n = 6 per group). (**F–J**) Representative the relative protein expression of GLUT1,GLUT3, HK2, LDHA and PDHA. All data were quantified by Image J software (n = 6 per group). Data are expressed as mean ± SD (post-hoc LSD test). #P < 0.05, ##P < 0.01, ###P < 0.001 vs Control group. *P < 0.05, **P < 0.01, ***P < 0.001 vs Model group.

regulation of small molecule metabolism, acetylcholine receptor signaling pathway, neurotransmitter receptor cycle. The involved MF included fatty acid binding, acetylcholine receptor activity, 3-methyl-2-oxy-butyrate dehydrogenase (acetyl transfer) kinase activity, etc (Figure 8B). Moreover, KEGG analysis revealed that JPZDD influenced various pathways, including the IL-17 signaling pathway, NF-κB signaling pathway, calcium signaling pathway, and PI3K-AKT signaling pathway, etc (Figure 8C). Intriguingly, the PI3K-AKT pathway was also identified through KEGG analysis in network pharmacology, underscoring its potential significance in the mechanism of action of JPZDD.

JPZDD Inhibited the PI3K/AKT/mTOR Pathway in Chronic Restraint Stress TS Rats

Integration of network pharmacology predictions with proteomics findings revealed the PI3K/AKT/mTOR signaling pathway as a potential target for the therapeutic action of JPZDD. This pathway is known to play a pivotal role in metabolism and inflammation regulation. Western blot analysis was performed to verify the pathway. Compared to the

https://doi.org/10.2147/DDDT.S505173

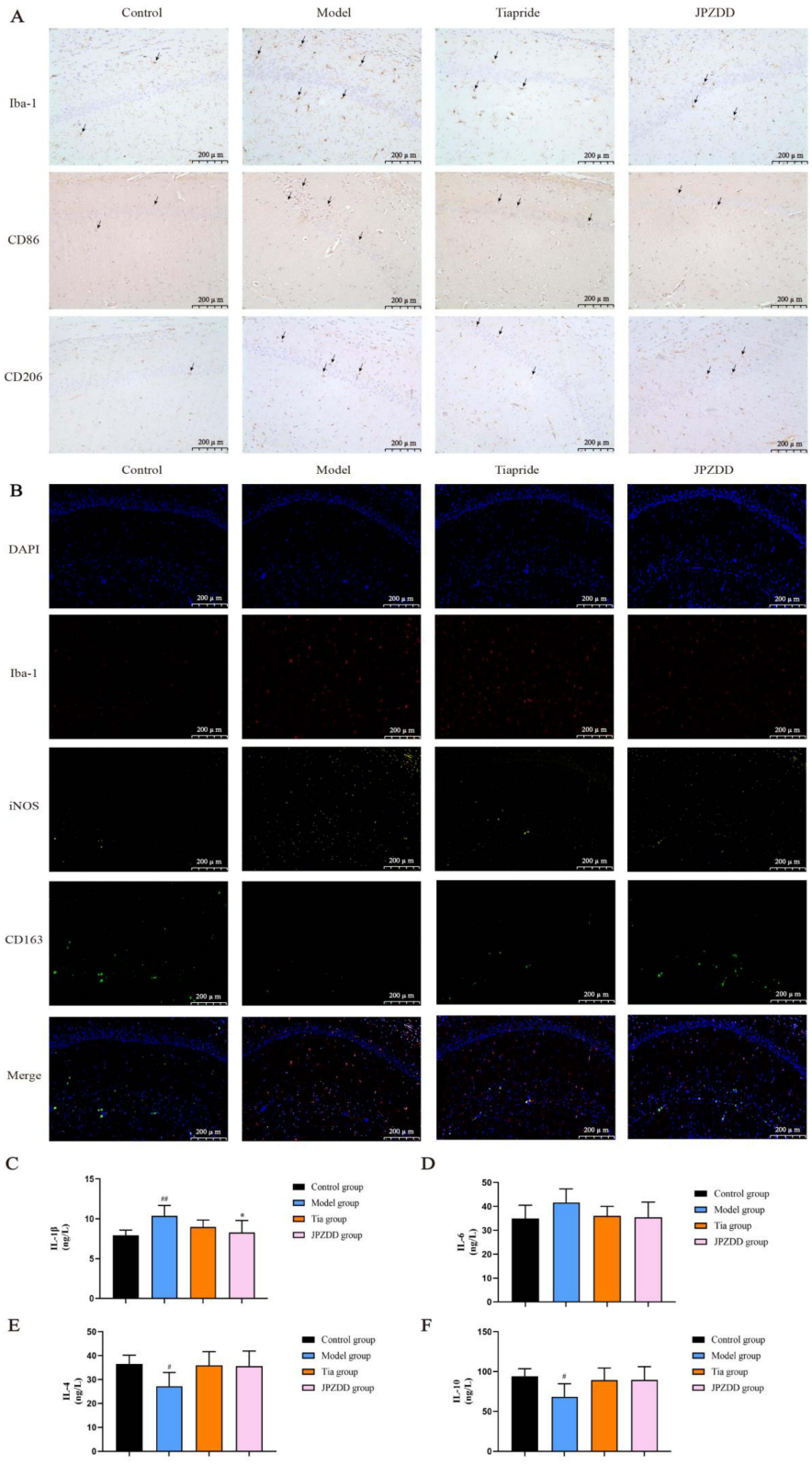

Figure 6 JPZDD regulates microglia polarization and inflammation. (**A**) Representative IHC Images of Iba-1, CD86 and CD206 proteins in the hippocampal tissues of different groups (arrows point to positive cells). (**B**) M1 and M2 cells were labeled with triple immunofluorescence staining. Cell nuclei were stained with DAPI (blue), microglia cells were stained with Iba-1 (red), M1 cells were stained with iNOS (yellow), M2 cells were stained with CD163 (green). (× 200, Scale bars = 200 μm, n = 4). (**C–F**) The levels of IL-1β, IL-6, IL-4, IL-10 in hippocampal tissues of different groups (n = 6 per group). Data are expressed as mean ± SD (post-hoc LSD test). #P < 0.05, ##P < 0.01 vs Control group. *P < 0.05 vs Model group.

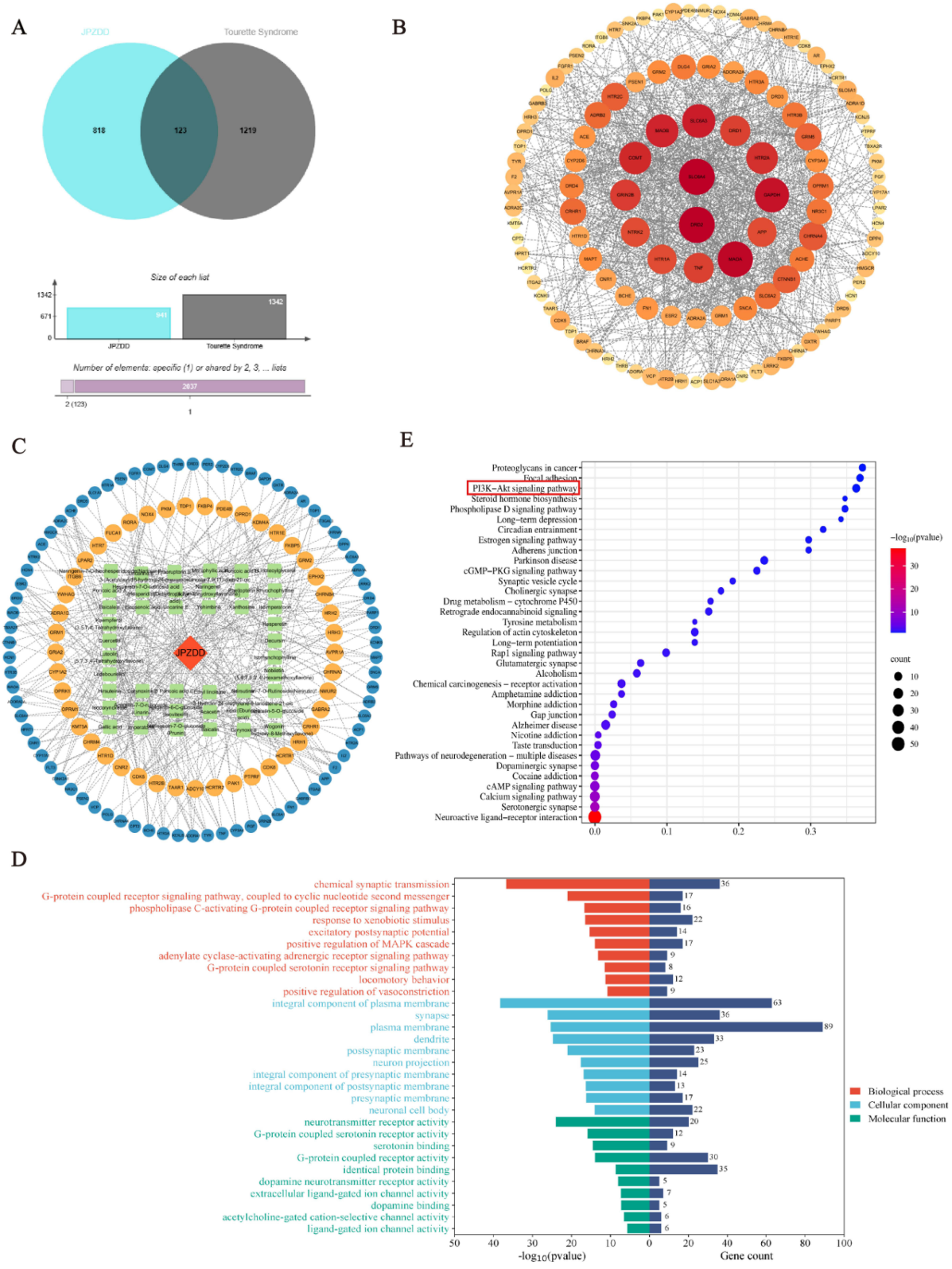

Figure 7 Network pharmacology analysis. (**A**) Venn diagram of 123 intersecting genes (JPZDD vs Tourette Syndrome). (**B**) PPI network of intersecting genes. (**C**) Composite target network of potential therapeutic targets for JPZDD. Yellow rhombus nodes indicate JPZDD; green rectangle nodes indicate active ingredients in JPZDD; blue and Orange circle nodes represent the potential targets. (**D**) The GO enrichment analysis of potential therapeutic targets. (**E**) The KEGG enrichment analysis of potential therapeutic targets.

https://doi.org/10.2147/DDDT.S505173

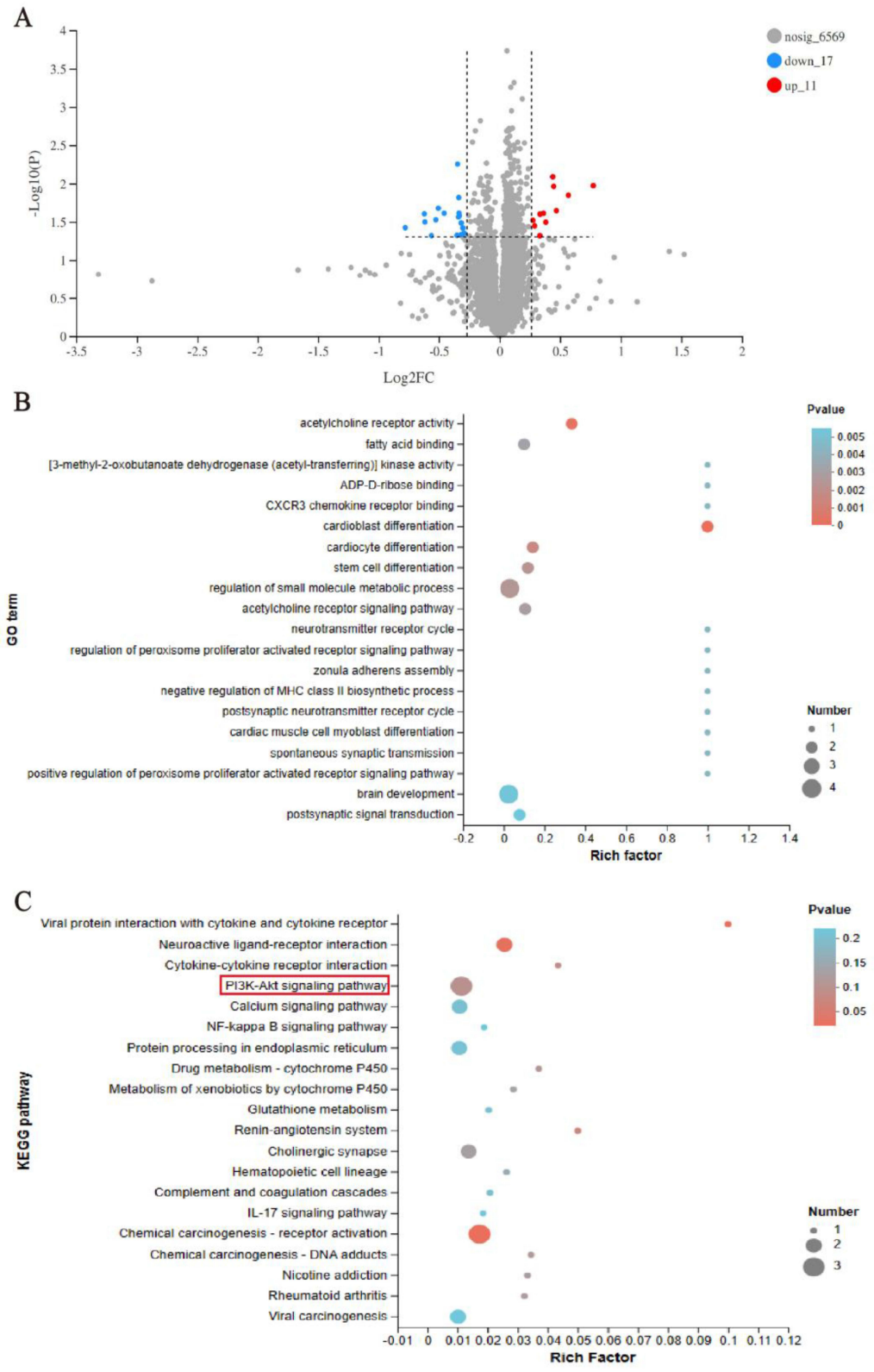

Figure 8 Proteomics analysis of the DEPs. (**A**) The volcano plot of the differential proteins (JPZDD group vs Model group). (**B**) The GO enrichment analysis of DEGs (JPZDD group vs Model group). (**C**) The KEGG enrichment analysis of DEGs (JPZDD group vs Model group).

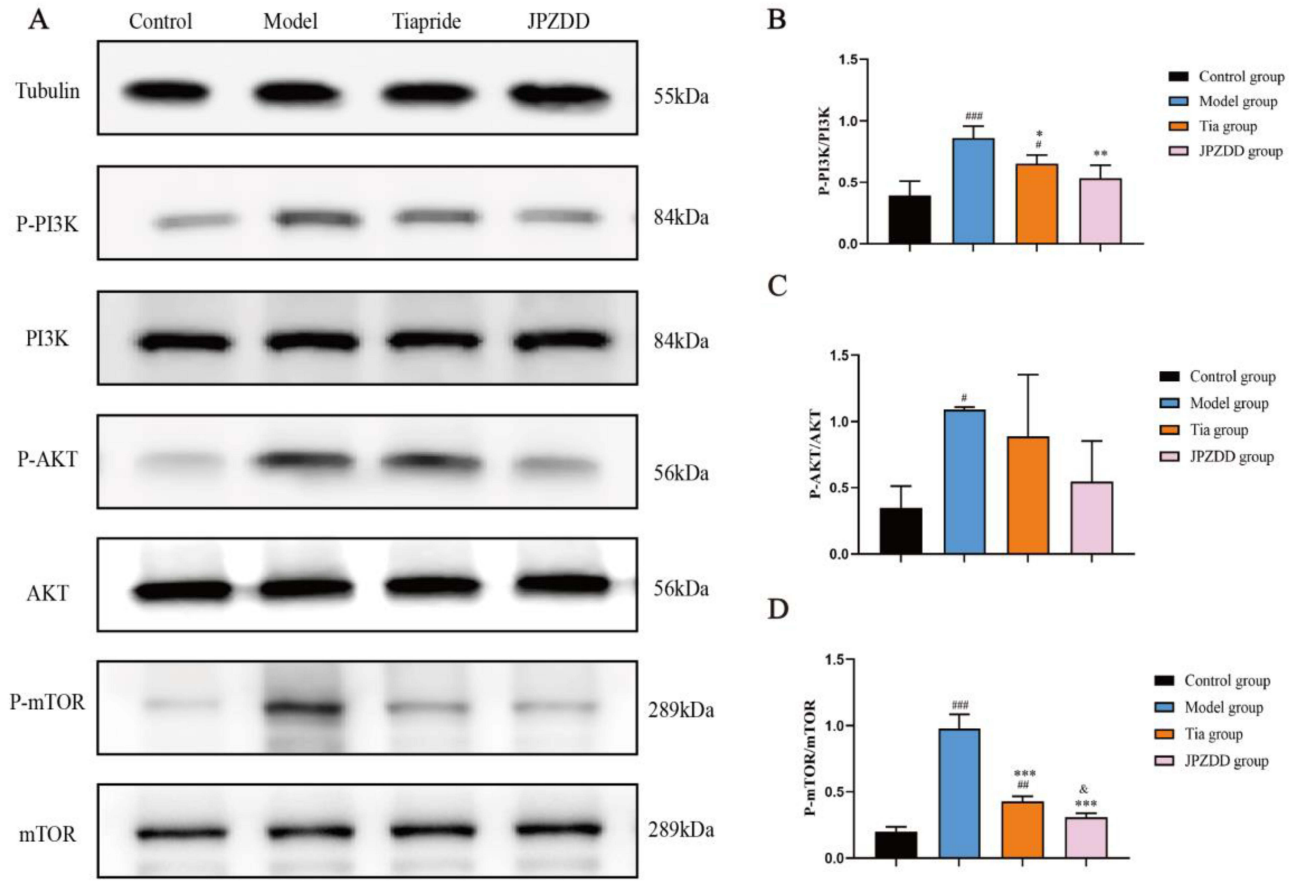

Figure 9 JPZDD could improve tic symptom by inhibiting PI3K/AKT/mTOR signaling pathway. (**A**) Protein expression levels of PI3K, AKT, mTOR, p-PI3K, p-AKT and p-mTOR. (**B–D**) Statistical analysis of phosphorylation and total protein levels of PI3K, AKT and mTOR. Data are expressed as mean ± SD (post-hoc LSD test). #P < 0.05, ##P < 0.01, ###P < 0.001 vs Control group. *P < 0.05, **P < 0.01, ***P < 0.001 vs Model group. and P < 0.05, vs Tia group.

control group, the model group exhibited significantly elevated phosphorylation levels of PI3K, AKT, and mTOR ($p < 0.05$). Conversely, the JPZDD group demonstrated significantly reduced phosphorylation levels of these proteins ($p < 0.05$) (Figure 9A–D). These results are consistent with the predictions from proteomics and network pharmacology, indicating that JPZDD may modulate microglia polarization, alleviate inflammation, and influence glucose metabolism by inhibiting the PI3K/AKT/mTOR signaling pathway, thus ameliorating tic symptoms (Figure 10).

Discussion

TS is a complex neuropsychiatric disease, which is sensitive to stress.2 The fact that stress increases the need for glucose to support neuronal transmission. When supply of glucose is insufficient, excitotoxicity ensues in the hippocampus.[26] Notably, microglia is also particularly sensitive to stress factors.[27] Changes in glucose metabolism are involved in the regulation of hippocampal neuroinflammation, potentially linking chronic stress and proinflammatory microglial activation.[28] The neuroinflammatory response hypothesis has gained traction in TS pathogenesis. Under different inflammatory conditions, microglia demonstrate distinct metabolic characteristics, with the manipulation of microglia metabolism capable of altering immune function, and potentially impacting neuroinflammatory disease progression. Microglia are able to switch their cell metabolism from mainly mitochondrial OXPHOS to glycolysis in response to pro-inflammatory stimuli.[29] Activated M1 phenotype rely on glycolytic metabolism to supply the pro-inflammatory activity, while oxidative phosphorylation (OXPHOS) would represent the main energy source of M2.[30] Hence, our hypothesis posits that the exacerbation or recurrence of TS induced by stress is intricately linked to the processes of microglial polarization and metabolic reprogramming.

https://doi.org/10.2147/DDDT.S505173

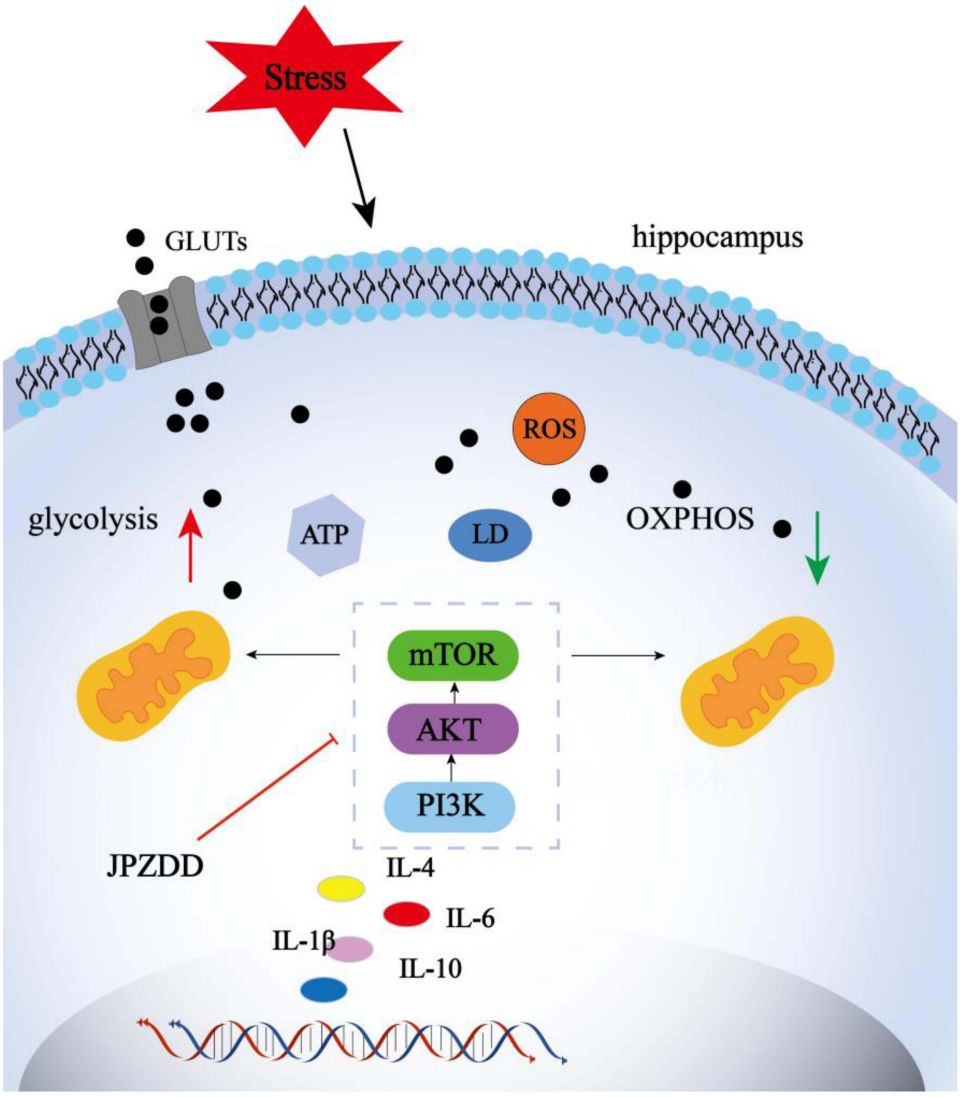

Figure 10 JPZDD could improve tic symptom by inhibiting PI3K/AKT/mTOR signaling pathway.

Our research has previously established chronic restraint stress TS model,[31] and the therapeutic effect of JPZDD on TS was revealed. Nonetheless, the specific mechanism remains incompletely elucidated. Through UPLC-MS/MS technology, this study further screened the effective components of JPZDD, each showcasing distinct pharmacological effects. For instance, gallic acid, Isovitexin and Linarin exerts anti-apoptotic, oxidative stress-regulating, and anti-inflammatory properties, thus aiding in cell function restoration.[32–34] Proleptin and hirsutine has been reported to regulating metabolic pathway and mitochondrial activity.[35,36] These findings suggest that the primary components of JPZDD potentially alleviate tic symptoms by modulating inflammation and regulating metabolism. Studies have demonstrated the neuroprotective effects of flavonoids, alkaloids, polysaccharides, and polyphenols found in major Chinese herbal medicines such as Scutellaria baicalensis (Huang Qin), Salvia miltiorrhiza (Dan Shen), Ligusticum chuanxiong (Chuan Xiong), and Gastrodia elata (Tian Ma). These compounds have shown significant anti-inflammatory, antioxidant, and neurogenic properties.[37]

In animal experiment, we observed that JPZDD could reduce the expressions of GLUT1 and GLUT3 in hippocampus. The transference of glucose from the bloodstream into brain cells is mediated by a family of proteins known as GLUTs. GLUT1 is pivotal, as it is tasked with the efficient translocation of glucose from the blood into the extracellular space of the brain's tissues. Neurons obtain glucose from extracellular environment for energy production mainly depending on

GLUT3. GLUT3 uptakes glucose with high affinity and great transport capacity, and is important for neuronal energy metabolism.[38] In principle, microglia express all the key enzymes implicated in the major metabolic pathways and a variety of glucose transporter proteins (GLUTs).[39,40] Stress upregulated GLUT1 expression in microglia. The increased GLUT1 level triggered by chronic stress may be associated with the high energy demand of activated microglia.[28] Modulating glycolytic metabolism by reducing glucose uptake through GLUT1 depletion effectively suppresses microglial activation and proinflammatory factor production.[8] In JPZDD group, glucose metabolizing enzymes and metabolites have differences compared with the model group. Glycolysis is controlled by HKs. Pyruvate's metabolic fate is controlled by PDHC and LDHA, and then, LDHA converts pyruvate to lactate.[11] Lactate, a key metabolite resulting from glycolysis, plays a crucial role in modulating the dialogue between glial cells and neurons. The process of microglial metabolic reprogramming, accompanied by an escalated secretion of lactate, has been identified to intensify inflammatory responses.[40,41] Key enzymes involved in glycolytic metabolism are shown to regulate microglial inflammatory responses and neuroinflammation, and down-regulating the expression of HK2 in microglia can inhibit the activation of microglia, improve their phagocytic function, reduce neuroinflammation and improve related neuropathology.[42,43] JPZDD has been demonstrated to attenuate neuroinflammation and modulate glucose metabolism, potentially through involvement in signaling pathways such as dopamine, although the precise mechanisms remain unclear.

In this study, network pharmacology results suggested that the PI3K/AKT/mTOR signaling pathway was modulated by JPZDD. To determine whether JPZDD could play the role of TS therapy by interfering with PI3K/AKT/mTOR signaling pathway, proteomics technology was employed to screen differential proteins in the hippocampal tissues of control, model, and JPZDD groups. Notably, the PI3K/AKT pathway displayed significant differences in KEGG enrichment analysis. The PI3K/AKT/mTOR pathway has been shown to be associated with neuroinflammation and energy metabolism. PI3K stimulates the activity of GLUT1 and vital glycolytic enzymes such as HK1, pyruvate kinase M2 and LDHA. PI3K/AKT signal is an essential effector of microglia glycolysis.[44] Meanwhile, PI3K/AKT signaling activates mammalian target of rapamycin (mTOR), which is a pivotal effector of metabolism in microglia.[45] In terms of mechanism, different metabolic regulators, such as LD, PI3K, mTOR can regulate the metabolism of immune cells.[46] Given previous evidence linking this pathway to neuroinflammation and energy metabolism, this study sought to determine JPZDD's impact on glucose metabolism and microglia polarization through the PI3K/AKT/mTOR pathway for alleviating tic symptoms. Western blot analysis validated distinctive protein expressions between the model and JPZDD groups, underscoring the targeted modulation of the PI3K/AKT/mTOR pathway by JPZDD.

In conclusion, JPZDD's potential in regulating microglia polarization, diminishing excessive inflammation, normalizing glucose metabolism, and alleviating tic symptoms through the inhibition of the PI3K/AKT/mTOR pathway presents a promising avenue for TS treatment. However, the current study has several limitations that warrant consideration. Given the inherent complexity of TCM preparations, future research should focus on elucidating the therapeutic mechanisms of TCM in treating tic disorders at both the monomer and component levels. From a statistical perspective, this study did not perform post-hoc analyses to further investigate the heterogeneity observed in the data. Subsequent research should incorporate a broader range of experimental approaches, including in vitro cell-based assays and clinical trials in human subjects, to validate and extend the findings of this study. Clarifying the potential role of the PI3K/AKT/mTOR signaling pathway as the link between microglial glucose metabolism and microglia polarization in TS will offer novel and effective treatment strategies for this condition.

Abbreviations

AOD, average optical density; BP, Biological process; CA, Cornus ammonics; CC, Cellular component; DA, dopamine; DG, Dentate gyrus; DL, Drug-likeness; GLU, glucose; GLUT, glucose transporter; GO, Gene ontology; HK2, Hexokinase II; HPA, Hypothalamic-pituitary-adrenal; Iba-1, Ionized calcium-binding adapter molecule 1; IDPN, Iminodipropionitrile; IL-10, Interleukin-10; IL-1β, Interleukin-1β; IL-4, Interleukin-4; IL-6, Interleukin-6; JPZDD, Jianpi Zhidong Decoction; KEGG, Kyoto Encyclopedia of Genes and Genomes; LD, Lactic Acid; LDHA, Lactate dehydrogenase A; MF, Molecular function; MG, Microglia; mTOR, mammalian target of rapamycin; OB, Oral bioavailability; OFT, open-field test; PDH, Prephenate dehydrogenase; PI3K, Phosphatidylinositol3-kinase; TCA, Tricarboxylic

acid cycle; TD, tic disorders; TS, Tourette Syndrome; TIC, Total ions current; UPLC-MS/MS, Ultra Performance Liquid Chromatography Tandem Mass Spectrometry.

Data Sharing Statement

Data will be made available on request.

Ethical Approval

Animal experiments were approved by Experimental Animal Welfare Ethics Committee, Institute of Basic Theory for Chinese Medicine, China Academy of Chinese Medical Sciences (No.220602). All research animals were used in compliance with the guidelines of Institutional Animal Care and Use Committee of Capital Medical University.

The human data part of our experiments is exempt from ethical review approval in accordance with national legislative guidelines, specifically Article 32 (1) and (2) of China's "Measures for the Ethical Review of Life Science and Medical Research Involving Human Subjects," dated February 18, 2023.

Informed Consent

Informed consent was written by all individual participants included in the study.

Author Contributions

All authors made a significant contribution to the work reported, whether that is in the conception, study design, execution, acquisition of data, analysis and interpretation, or in all these areas; took part in drafting, revising or critically reviewing the article; gave final approval of the version to be published; have agreed on the journal to which the article has been submitted; and agree to be accountable for all aspects of the work.

Funding

This study received support from several funding sources: National Natural Science Foundation of China (No.82374520).

Disclosure

The authors have declared that no competing interests exist in this work.

References

1. Li F, Cui Y, Li Y, et al. Prevalence of mental disorders in school children and adolescents in China: diagnostic data from detailed clinical assessments of 17,524 individuals. *J Child Psychol Psychiatr*. 2022;63(1):34–46. doi:10.1111/jcpp.13445
2. Johnson KA, Worbe Y, Foote KD, et al. Tourette syndrome: clinical features, pathophysiology, and treatment. *Lancet Neurol*. 2023;22(2):147–158. doi:10.1016/S1474-4422(22)00303-9
3. Jiang J, Chen M, Huang H, et al. The aetiology of Tourette syndrome and chronic tic disorder in children and adolescents: a comprehensive systematic review of case-control studies. *Brain Sci*. 2022;12(9):1202. doi:10.3390/brainsci12091202
4. Alongi P, Iaccarino L, Perani D. PET neuroimaging: insights on dystonia and tourette syndrome and potential applications. *Front Neurol*. 2014;5:183. doi:10.3389/fneur.2014.00183
5. Frick L, Pittenger C. Microglial dysregulation in OCD, Tourette syndrome, and PANDAS. *J Immunol Res*. 2016;2016:8606057. doi:10.1155/2016/8606057
6. Bielanin JP, Sun D. Significance of microglial energy metabolism in maintaining brain homeostasis. *Transl Stroke Res*. 2023;14(4):435–437. doi:10.1007/s12975-022-01069-6
7. Cao W, Feng Z, Zhu D, et al. The role of PGK1 in promoting ischemia/reperfusion injury-induced Microglial M1 polarization and inflammation by regulating glycolysis. *Neuromol Med*. 2023;25(2):301–311. doi:10.1007/s12017-023-08736-3
8. Cheng J, Zhang R, Xu Z, et al. Early glycolytic reprogramming controls microglial inflammatory activation. *J Neuroinflammation*. 2021;18(1):129. doi:10.1186/s12974-021-02187-y
9. Lynch MA. Can the emerging field of immunometabolism provide insights into neuroinflammation? *Prog Neurobiol*. 2020;184:101719. doi:10.1016/j.pneurobio.2019.101719
10. Yang S, Qin C, Hu ZW, et al. Microglia reprogram metabolic profiles for phenotype and function changes in central nervous system. *Neurobiol Dis*. 2021;152:105290. doi:10.1016/j.nbd.2021.105290
11. Xu S, Deng KQ, Lu C, et al. Interleukin-6 classic and trans-signaling utilize glucose metabolism reprogramming to achieve anti- or pro-inflammatory effects. *Metabolism*. 2024;155:155155832. doi:10.1016/j.metabol.2024.155832
12. Orihuela R, McPherson CA, Harry GJ. Microglial M1/M2 polarization and metabolic states. *Br J Pharmacol*. 2016;173(4):649–665. doi:10.1111/bph.13139

13. Häge A, Krämer R, Dunlap M, et al. Emerging therapeutic approaches for Tourette syndrome and other tic disorders - a systematic review of current clinical trials. *Eur Child Adolesc Psychiatry*. 2024. doi:10.1007/s00787-024-02637-x
14. Cui X, Yu WJ, Zhang W, et al. Effects of Jian-Pi-Zhi-Dong decoction on hypothalamic pituitary adrennal axis of children with Tourette syndrome. *Modern Chin Clin Med*. 2016;23(06):17–20.
15. Miao CX, Wei XH, Hu KQ, Tan LQ. Effect of Using Jianpi Zhidong decoction combined with western medicine in the treatment of multiple tic with abnormal EEG. *J Sichuan Trad Chin Med*. 2021;39(01):137–140.
16. Wang YJ. Effect of Jianpi Zhidong Decoction combined with aripiprazole in improving muscle function and behavioral abnormality in children with pediatric multiple tics. *J Clin Med Pract*. 2024;28(8):104–108.
17. Yu WJ, Bai X, Zhang W, Wei L, Shi XW, Wang SM. Effects of Jianpi Zhidong decoction on the neurotransmitters of tourette syndrome children. *China J Tradition Chinese Med Pharm*. 2015;30(05):1757–1761.
18. Kang B, Chen Y. Effects of Jianpi Zhidong decoction combined with auricular point sticking on hypothalamic-pituitary-adrenal axis and neurotransmitter content of children with tourette syndrome. *World Chin Med*. 2019;14(06):1524–1527+1531.
19. Bai X, Zhang HX, Zhou QQ, et al. Effects of Jianpi Zhidong decoction on prefrontal cortex neurons and neurotrophic factors in rats with chronic restraint stress tic disorder. *Global Tradit Chin Med*. 2022;15(06):991–995.
20. Zhang W, Yu W, Liu X, et al. Effect of Jian-Pi-Zhi-Dong decoction on the amino acid neurotransmitters in a rat model of tourette syndrome and comorbid anxiety disorder. *Front Psychiatry*. 2020;11:515. doi:10.3389/fpsyt.2020.00515
21. Zhang N, Cui X, Zhang HX, et al. Study on the effect and mechanism of Jianpi Zhidong decoction on glucose metabolism chronic in restraint stress Tourette syndrome model. *China J Tradition Chinese Med Pharm*. 2024;39(05):2522–2526.
22. Wang DH, Li W, Liu XF, Zhang JM, Wang SM. Chinese medicine formula "Jian-Pi-Zhi-Dong Decoction" attenuates Tourette syndrome via down-regulating the expression of dopamine transporter in mice. *Evid Based Complement Alternat Med*. 2013;2013:385685. doi:10.1155/2013/385685
23. Zhang W, Wei L, Yu W, et al. Effect of Jian-Pi-Zhi-Dong decoction on striatal glutamate and gamma-aminobutyric acid levels detected using microdialysis in a rat model of Tourette syndrome. *Neuropsychiatr Dis Treat*. 2016;12:1233–1242. doi:10.2147/NDT.S106330
24. Khan HA, Alhomida AS, Arif IA. Neurovestibular toxicities of acrylonitrile and iminodipropionitrile in rats: a comparative evaluation of putative mechanisms and target sites. *Toxicol Sci*. 2009;109(1):124–131. doi:10.1093/toxsci/kfp043
25. Daina A, Michielin O, Zoete V. SwissTargetPrediction: updated data and new features for efficient prediction of protein targets of small molecules. *Nucleic Acids Res*. 2019;47(W1):W357–W364. doi:10.1093/nar/gkz382
26. Osborne DM, Pearson-Leary J, McNay EC. The neuroenergetics of stress hormones in the hippocampus and implications for memory. *Front Neurosci*. 2015;9:164. doi:10.3389/fnins.2015.00164
27. Sugama S, Kakinuma Y. Stress and brain immunity: microglial homeostasis through hypothalamus-pituitary-adrenal gland axis and sympathetic nervous system. *Brain Behav Immun Health*. 2020;7:100111. doi:10.1016/j.bbih.2020.100111
28. Wang X, Wu Y, Tian Y, et al. GLUT1-mediated microglial proinflammatory activation contributes to the development of stress-induced spatial learning and memory dysfunction in mice. *Cell Biosci*. 2024;14(1):48. doi:10.1186/s13578-024-01229-1
29. Sabogal-Guaqueta AM, Marmolejo-Garza A, Trombetta-Lima M, et al. Species-specific metabolic reprogramming in human and mouse microglia during inflammatory pathway induction. *Nat Commun*. 2023;14(1):6454. doi:10.1038/s41467-023-42096-7
30. Sangineto M, Ciarnelli M, Cassano T, et al. Metabolic reprogramming in inflammatory microglia indicates a potential way of targeting inflammation in Alzheimer's disease. *Redox Biol*. 2023;66:102846. doi:10.1016/j.redox.2023.102846
31. Zhang HX, Guo F, Zhang W, Yao N, Zhou QQ, Cui X. Evaluation of the influence of chronic restraint stress simulated emotional factors on the rat model of Tourette syndrome. *China J Trad Chin Med Pharm*. 2021;21(36(03)):1383–1388.
32. Mansouri MT, Farbood Y, Sameri MJ, et al. Neuroprotective effects of oral gallic acid against oxidative stress induced by 6-hydroxydopamine in rats. *Food Chem*. 2013;138(2–3):1028–1033. doi:10.1016/j.foodchem.2012.11.022
33. Hao R, Li M, Li F, et al. Protective effects of the phenolic compounds from mung bean hull against H(2)O(2)-induced skin aging through alleviating oxidative injury and autophagy in HaCaT cells and HSF cells. *Sci Total Environ*. 2022;841:156669. doi:10.1016/j.scitotenv.2022.156669
34. Wang L, Wang J, Ren G, et al. Ameliorative effects of the Coptis inflorescence extract against lung injury in diabetic mice by regulating AMPK/NEU1 signaling. *Phytomedicine*. 2023;118:154963. doi:10.1016/j.phymed.2023.154963
35. Liu X, Chen DW, Wu X, et al. The inhibition of UDP-glucuronosyltransferase (UGT) isoforms by praeruptorin A and B. *Phytother Res*. 2016;30(11):1872–1878. doi:10.1002/ptr.5697
36. Jiang W, Zhang Y, Zhang W, et al. Hirsutine ameliorates myocardial ischemia-reperfusion injury through improving mitochondrial function via CaMKII pathway. *Clin Exp Hypertens*. 2023;45(1):2192444. doi:10.1080/10641963.2023.2192444
37. Meng W, Chao W, Kaiwei Z, et al. Bioactive compounds from Chinese herbal plants for neurological health: mechanisms, pathways, and functional food applications. *Front Nutr*. 2025;12:1537363. doi:10.3389/fnut.2025.1537363
38. Peng W, Tan C, Mo L, et al. Glucose transporter 3 in neuronal glucose metabolism: health and diseases. *Metabolism*. 2021;123:154869. doi:10.1016/j.metabol.2021.154869
39. Jurcovicova J. Glucose transport in brain - effect of inflammation. *Endocr Regul*. 2014;48(1):35–48. doi:10.4149/endo_2014_01_35
40. Monsorno K, Buckinx A, Paolicelli RC. Microglial metabolic flexibility: emerging roles for lactate. *Trends Endocrinol Metab*. 2022;33(3):186–195. doi:10.1016/j.tem.2021.12.001
41. Hua T, Kong E, Zhang H, et al. PRMT6 deficiency or inhibition alleviates neuropathic pain by decreasing glycolysis and inflammation in microglia. *Brain Behav Immun*. 2024;118:101–114. doi:10.1016/j.bbi.2024.02.027
42. Li Y, Lu B, Sheng L, et al. Hexokinase 2-dependent hyperglycolysis driving microglial activation contributes to ischemic brain injury. *J Neurochem*. 2018;144(2):186–200. doi:10.1111/jnc.14267
43. Wang S, Jiang C, Cao K, et al. HK2 in microglia and macrophages contribute to the development of neuropathic pain. *Glia*. 2024;72(2):396–410. doi:10.1002/glia.24482
44. Wang Q, Lu M, Zhu X, et al. The role of microglia immunometabolism in neurodegeneration: focus on molecular determinants and metabolic intermediates of metabolic reprogramming. *Biomed Pharmacother*. 2022;153:113412. doi:10.1016/j.biopha.2022.113412
45. Biswas SK. Metabolic reprogramming of immune cells in cancer progression. *Immunity*. 2015;43(3):435–449. doi:10.1016/j.immuni.2015.09.001
46. Xiang H, Yang R, Tu J, et al. Metabolic reprogramming of immune cells in pancreatic cancer progression. *Biomed Pharmacother*. 2023;157:113992. doi:10.1016/j.biopha.2022.113992